Electronic Supplementary Material (ESI) for CrystEngComm.

Supporting Information

P-n junctions in planar GaAs nanowires

Bogdan R. Borodin[1], Prokhor A. Alekseev[1,], Vladislav Khayrudinov[2], Evgeniy Ubyivovk[3], Yury Berdnikov[3], Nickolay Sibirev[3], Harri Lipsanen[2]*

[1] Ioffe Institute, 194021 Saint Petersburg, Russia

[2] Department of Electronics and Nanoengineering, Micronova, Aalto University, 00076 Espoo, Finland

[3] Saint Petersburg State University, 198504 Saint Petersburg, Russia

E-mail: [*]npoxep@gmail.com

S1. Calculation of the chemical potential difference for the oscillation of the NW diameter during the growth

The NW growth rate W is determined by the difference of chemical potentials in the liquid and solid phases per pair of Ga-As atoms, which we denote as $\Delta\mu$.[1,2] It can be calculated using Redlich-Kister formalism[3,4] as

$$\Delta\mu = k_B T ln(C_{Ga}) + k_B T ln(C_{As}) + \omega_{GaAs} {C_{As}}^2 + \omega_{GaAs} {C_{Ga}}^2 + \sum_\gamma \big(\omega_{\gamma Ga} {C_\gamma}^2 + \big(\omega_{GaAs} + \omega_{\gamma Ga} - \omega_{\gamma As}\big) C_\gamma C_{As} + \omega_{\gamma As} {C_\gamma}^2 + \big(\omega_{GaAs} + \omega_{\gamma As} - \omega_{\gamma Ga}\big) C_\gamma C_{Ga}\big), \quad \text{(S1)}$$

where C_α is the concentration of corresponding element in the catalyst droplet and $\omega_{\alpha\beta}$ denotes the binary coefficients (with $\alpha, \beta = Ga, As, Au, Zn, Sn$), $k_B$is the Boltzmann constant and T is the growth temperature. Index γ = Au, Zn, Sn in the sum in the right-hand side of eq. (s1). Therefore, the derivatives M and G defined in the main text could be found as

$$M = \frac{S}{\Omega_{GaAs}} \frac{\partial}{\partial N_{Ga}} W = \frac{S}{\Omega_{GaAs}} \frac{\partial W}{\partial \Delta\mu} \frac{\partial C_{Ga}}{\partial N_{Ga}} \Big(k_B T \frac{1}{C_{Ga}} + 2\omega_{GaAs} C_{Ga} + \sum_\gamma \big(\omega_{GaAs} + \omega_{\gamma As} - \omega_{\gamma Ga}\big) C_\gamma \Big), \quad \text{(S2)}$$

and

$$G = \frac{S}{\Omega_{GaAs}} \frac{\partial}{\partial N_{As}} W = \frac{S}{\Omega_{GaAs}} \frac{\partial W}{\partial \Delta\mu} \frac{\partial C_{As}}{\partial N_{As}} \Big(k_B T \frac{1}{C_{As}} + 2\omega_{GaAs} C_{As} + \sum_\gamma \big(\omega_{GaAs} + \omega_{\gamma Ga} - \omega_{\gamma As}\big) C_\gamma \Big). \quad \text{(S3)}$$

Then we calculate the derivatives of Ga and As concentrations as $\partial C_{Ga}/\partial N_{Ga} = (1 - C_{Ga})/N_{tot}$ and $\partial C_{As}/\partial N_{As} = (1 - C_{As})/N_{tot}$ and thus arrive to:

$$M + G = \frac{1}{N_{tot}} \frac{S}{\Omega_{GaAs}} \frac{\partial W}{\partial \Delta\mu} \Big(k_B T \frac{1 - C_{Ga}}{C_{Ga}} + k_B T \frac{1 - C_{As}}{C_{As}} + \omega_{GaAs}(2 - C_{Ga} - C_{As}) - \omega_{GaAs}(C_{Ga} - C_{As})^2 + (C_{As} - C_{Ga}) \sum_\gamma \big(\omega_{\gamma As} - \omega_{\gamma Ga}\big) C_\gamma \Big) \quad \text{(S4)}$$

Assuming the concentration of gold and dopant elements in the droplet to be considerably smaller than $C_{Ga} + C_{As} \approx 1$ during the growth of planar segment, we neglect the terms proportional to C_γ (with γ = Au, Zn, Sn) and obtain

$$M + G \sim \frac{1}{N_{tot}} \frac{S}{\Omega_{GaAs}} \frac{\partial W}{\partial \Delta\mu} \Big[k_B T \Big(\frac{1 - C_{Ga}}{C_{Ga}} + \frac{1 - C_{As}}{C_{As}} \Big) + \omega_{GaAs} \big((2 - C_{Ga} - C_{As}) - (C_{Ga} - C_{As})^2 \big) \Big] \quad \text{(S5)}$$

Since the growth rate is monotonously growing function of $\Delta\mu$, $M + G < 0$ when the expression in the square brackets in the right-hand side of eq. (S5) is negative:

$$\frac{C_{As}}{1-C_{As}} + \frac{1-C_{As}}{C_{As}} + \frac{\omega_{GaAs}}{k_B T}(2 - (1-2C_{As})^2) < 0 \quad \text{(S6)}$$

The growth temperature in our experiment 470 °C gives $\frac{\omega_{GaAs}}{k_B T} = -4.65$ [3,5] and the fulfilment of the condition (S6) when C_{As} is between 0.24 and 0.76.

Next, we estimate the values of *M*, *G* and *E*. The derivative of gallium concentration could be written as $\partial C_{Ga}/\partial N_{Ga} = (1 - C_{Ga})\Omega_{GaAs}/V_{cat}$, where V_{cat} is the catalyst droplet volume. It allows to rewrite (S2), (S3) and (S4) in the form

$$M = \frac{S}{V_{cat}} \frac{\partial W}{\partial \Delta\mu} k_B T \left(\frac{(1-C_{Ga})}{C_{Ga}} + \frac{2\omega_{GaAs}}{k_B T} C_{Ga}(1 - C_{Ga}) \right), \quad \text{(S7)}$$

$$G = \frac{S}{V_{cat}} \frac{\partial W}{\partial \Delta\mu} k_B T \left(\frac{(1-C_{As})}{C_{As}} + \frac{2\omega_{GaAs}}{k_B T} C_{As}(1 - C_{As}) \right). \quad \text{(S8)}$$

$$M + G = \frac{S}{V_{cat}} \frac{\partial W}{\partial \Delta\mu} k_B T \left(\frac{(1-C_{Ga})}{C_{Ga}} + \frac{(1-C_{As})}{C_{As}} + \frac{2\omega_{GaAs}}{k_B T} C_{Ga}(1 - C_{Ga}) + \frac{2\omega_{GaAs}}{k_B T} C_{As}(1 - C_{As}) \right) \quad \text{(S9)}$$

The first factor in the right-hand side of (S9) is the ratio of planar nanowire cross-section area and the droplet volume. Thus, this factor is about one over droplet radius or planar segment width $S/V_{cat} \approx 1/100\, nm^{-1}$. The second factor $\frac{\partial W}{\partial \Delta\mu} \gtrsim \frac{3nm/s}{150\, meV}$ can be estimated using the previous calculations[2] of NW growth rates with respect to chemical potential difference. Growth temperature in our experiments is equivalent to $k_B T$ = 64 meV. So, the factors before parentheses together are about $1/100\, s^{-1}$. The sum in the parentheses varied from $2 + \omega_{GaAs}/k_B T \approx -2$ to infinity.

The value of *E* can be calculated as:

$$E = -\frac{1}{\tau}\frac{r_{As}}{R} + JA \frac{\partial}{\partial N_{As}} \left(ln\left(\frac{A}{{r_{As}}^2} \right) \right). \quad \text{(S10)}$$

The first term the includes the ratio of arsenic atomic radius r_{As} and the width of planar nanowire segment R. At the considered growth temperatures, the characteristic As desorption time is greater 1s, thus the first term in (S10) is about 10^{-3}.

The second term in (S10) is the derivative of arsenic incoming flux from vapor phase. Material balance requires the mean incoming flux to be equal to the sum of arsenic consumption via crystallization and evaporation. Thus, to estimate the order of magnitude we could said, that $JA \approx W$~10nm/s. The droplet surface area could be estimated as $A = C_g {N_{tot}}^{2/3} {r_{As}}^2$, where C_g is geometrical factor, so $\frac{\partial}{\partial N_{As}}\left(ln\left(\frac{A}{{r_{As}}^2}\right)\right) \approx \frac{2}{3N_{tot}}$. Total number of atoms N_{tot} in the catalyst droplet is extremely large number, even number of gold atoms in initial gold particle is about $3 \cdot 10^7$. So, the second term is negligible compared to the first one. Therefore, the quantity E is about 10^{-3} and the sign of $M + G - E$ is mainly determined by $M + G$ which is typically 10 times larger than E for the studied NW growth conditions.

Therefore, neglecting the interaction of Ga and As with the doping species inside the droplet, the criteria for droplet volume oscillations (eq. (4) of the main text) can be formulated as:

$$\left(\frac{1-C_{Ga}}{C_{Ga}} + \frac{1-C_{As}}{C_{As}}\right) + \frac{\omega_{GaAs}}{k_B T}(2 - C_{Ga} - C_{As} - (C_{Ga} - C_{As})^2) < 0, \qquad \text{(S11)}$$

which is reproduced in eq. (6) of the main text.

Direct measurement of the droplet composition during the NW growth is rare and only possible when the very sophisticated systems for in-situ growth monitoring are in use. For widely studied growth of vertical Au-catalyzed[1,6] or self-catalyzed[2] GaAs NWs, As concentration is generally found to be below 3%. However, no direct measurements were on Zn or Sn doped NW were reported so far. However, some qualitative estimations can rely on the analysis of the catalyst composition after the growth termination. Previous work reports the increase of the As and

decrease of Ga concentrations with the increase of the Zn doping flux[7] leading to similar concentrations of Ga and As at high level of Zn-doping of GaAs NWs. Moreover, As concentration in Sn-catalyzed GaAs NWs were found to be greater than Ga and could reach even one fifth of the droplet.[8]

According to our measurements after growth the droplet composition of Sn-doped nanowire is following: Au 80%, Ga 15%, As 4% and traces of Sn. Also, we measure the droplet composition of Zn-doped nanowire: Au 80%, Ga 12%, As 4% and Zn 3%. Surely, such compositions cannot be during the growth since chemical potential difference would be below zero and droplet should dissolve NW. However, since the NWs mainly consist of Ga and As, the concentrations of these atoms are expected to be higher during the growth and decrease during the cooling down for growth termination. Thus, our measurements are consistent with the elevated As concentration as the reason for droplet volume oscillations.

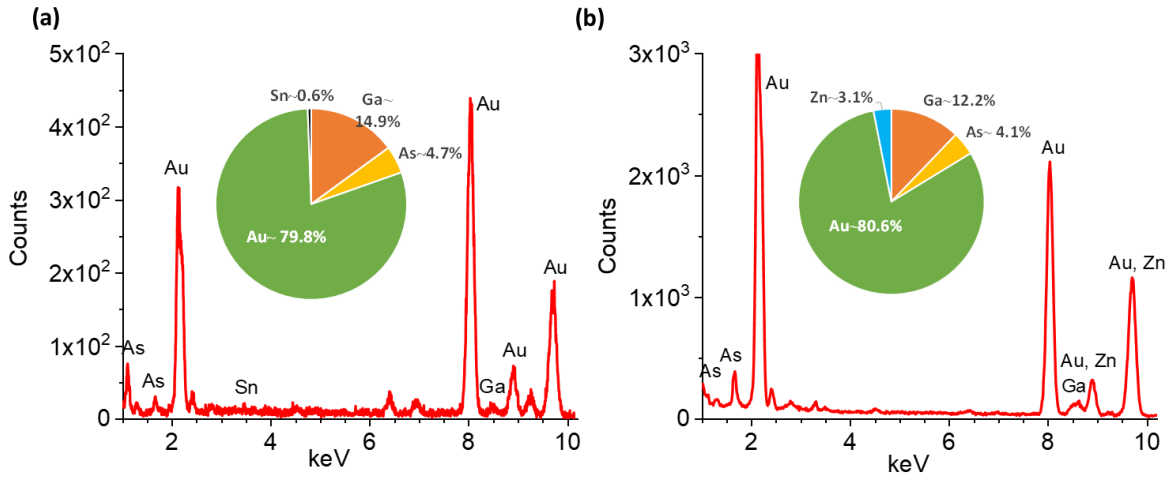

Figure S1. EDX spectrum of and Sn-doped NW droplet and of Zn-doped NW droplet

S2. C-AFM measurements for “p/n-p”, “n/n-p” and “p/no doping” samples

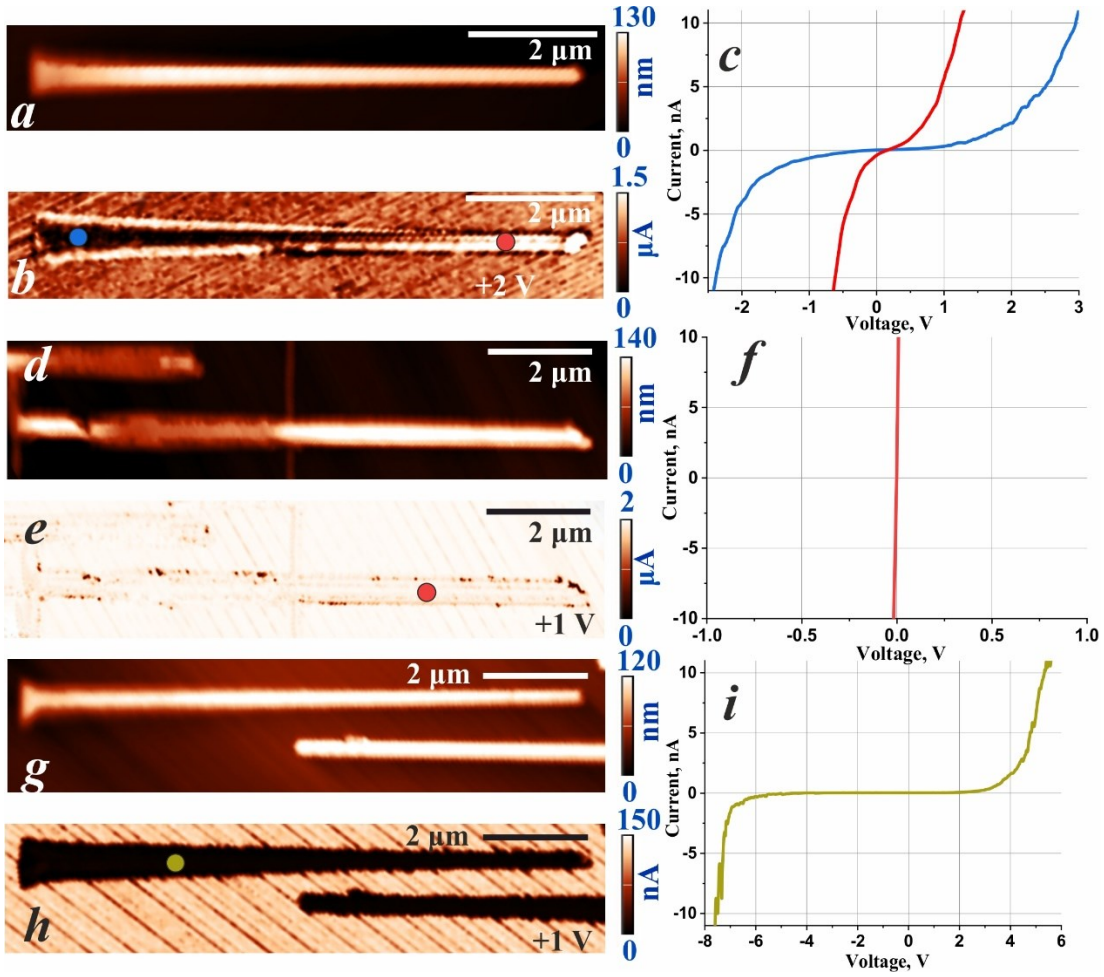

Figure S2. Topography, current maps, and I-V curves of nanowires. (a-c) p/n-p sample; (d-f) n/n-p sample; (g-i) p/no doping sample.

The red curve in Figure S2(c) is sublinear because the p-doped nanowire segment was grown on the p-doped substrate covered with the thin n-doped layer formed in the first stage of growth (when the n-doped segment was formed). The presence of this thin n-doped layer decreases conductivity and results in the sublinear shape. The blue curve in Figure S2(c) is rectifying because of the p-n junction formed between the p-doped substrate and the n-doped nanowire core. In Figure S2(e) the current map of the n/n-p sample is presented. The entire map is bright with monotonous conductivity. Figure S2(f) confirms the high conductivity. Such a case can emerge when the entire

surface is covered with the perfectly conductive p-doped layer. The presence of p-n junction between the p-doped layer and the n-doped substrate does not affect the conductivity because the highly conductive p-doped layer provides so large contact between the layers that its resistivity is negligible compared to the resistivity of the point contact between the probe and surface. Thus, the I-V curve characterizes only the resistivity of the contact. Figure S2(i) indicates the low conductivity of undoped nanowires.

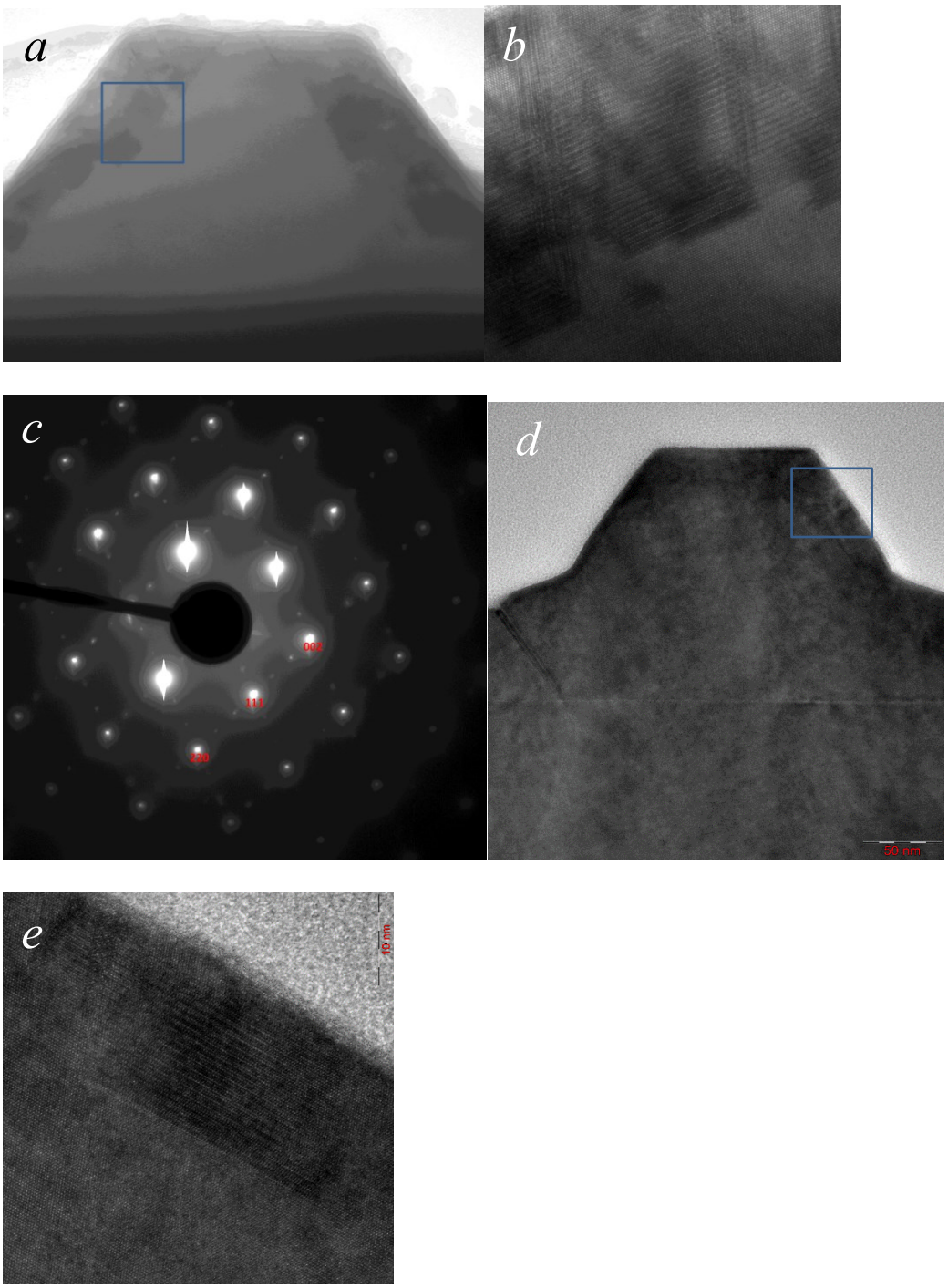

Figure S3. (a-c) Cross section of the p/p-n NW. (a) TEM image. (b) High resolution TEM image of the are marked by the blue frame in (a). (c) Diffraction pattern obtained corresponding to the (a). (d-e) Cross section of the n/p-n NW. (d) TEM image. (e) High resolution TEM image of the are marked by the blue frame in (d).

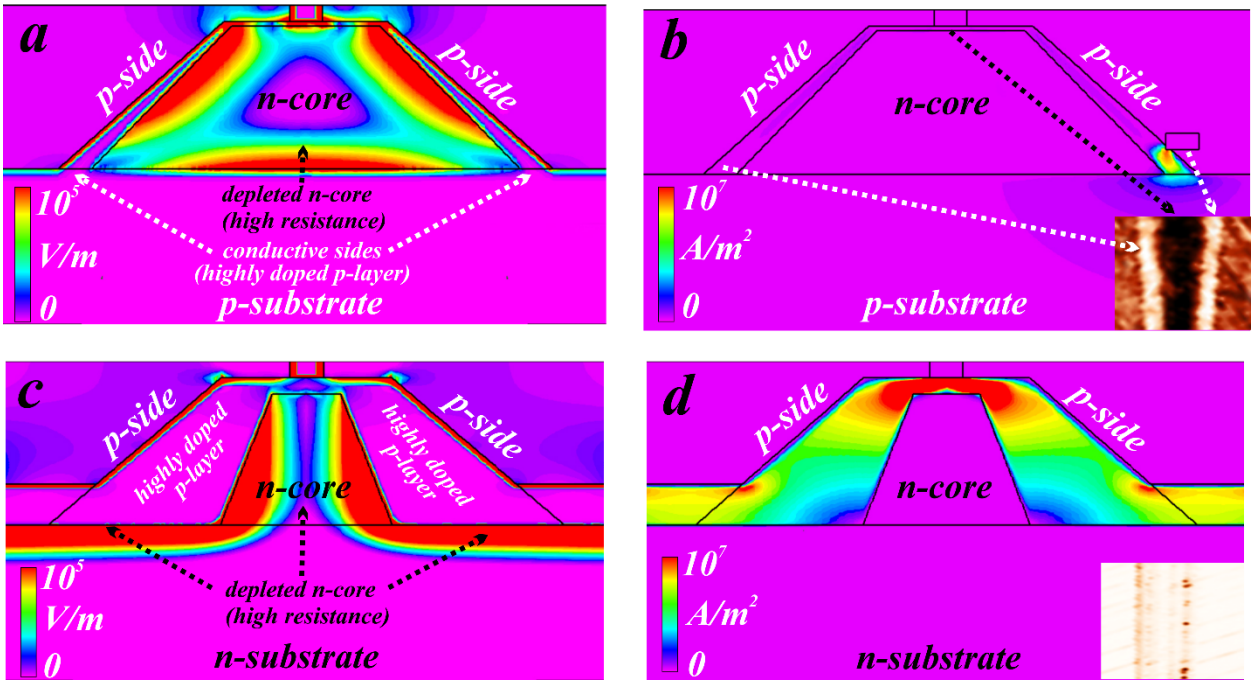

Figure S4. (*a, c*) Electric field and (*b, d*) current density distribution inside of p/n-p and n/n-p samples, respectively. The inserts are pieces of current maps from Figure 5.

Figure S2(a, b) shows AFM data for the p/n-p sample. As you can see the core of the nanowire is non-conductive, while the sides are conductive. The end of the nanowire is also conductive. At the beginning of growth, an n-doped core was formed, then the p-doped sides and the end grew. The relatively low-doped n-core is highly depleted and has a high resistance. While the depth of depletion in the high-doped p-layer covering this sample is small. Thus, in regions of maximum thickness, the p-layer turns out to be thicker than the depleted region, and conductive edges are observed. Figure S4 (a, b) shows the modeling results for the p/n-p sample. As can be seen from Figure S4a, the n-doped core of the nanowire is severely depleted, and it also depletes the thin p-layer around it. Thus, in regions of the minimum thickness of the p-layer (on the top of the nanowire), no conductivity is observed. At the same time, it can be seen from the distribution of the field that as you move away from the top, the width of the p-doped sides becomes larger than

the depletion. This means that such edges are conductive. Thus, the modeling is in good agreement with the experiment and the parameters of the structure are selected correctly.

Figure S2(d, e) shows AFM data for the n/n-p sample. The current map of this sample does not have explicit p-n transitions. The nanowire and surface are equally conductive. There are ragged non-conductive inclusions along the edges of the nanowire. In this sample, the surface layer is quite thick. Thus, a thick, not depleted, highly doped p-layer connects the surface of the nanowire to the substrate, and uniform conductivity is observed. Figure S4 (c, d) shows the modeling results for the n/n-p sample. As can be seen from Figure S4c, the n-doped core of the nanowire is severely depleted and its resistance is high. A depleted region is also formed at the boundary of the p-surface layer and the n-substrate. But since the entire surface is covered with a highly doped p-layer, this connects the wire to the surface. The modeling shows the flow of current through the surface p-doped layer (see Figure S4d), and it is in good agreement with the experiment.

References

(1) Glas, F. Chemical Potentials for Au-Assisted Vapor-Liquid-Solid Growth of III-V Nanowires. *J. Appl. Phys.* **2010**, *108* (7), 073506.

(2) Glas, F.; Ramdani, M. R.; Patriarche, G.; Harmand, J. C. Predictive Modeling of Self-Catalyzed III-V Nanowire Growth. *Phys. Rev. B - Condens. Matter Mater. Phys.* **2013**, *88* (19), 1–14.

(3) Ansara, I.; Chatillon, C.; Lukas, H. L.; Nishizawa, T.; Ohtani, H.; Ishida, K.; Hillert, M.; Sundman, B.; Argent, B. B.; Watson, A.; Chart, T. G.; Anderson, T. A Binary Database for III–V Compound Semiconductor Systems. *Calphad* **1994**, *18* (2), 177–222.

(4) Dinsdale, A. T. SGTE Data for Pure Elements. *Calphad* **1991**, *15* (4), 317–425.

(5) Li, C.; Li, J. B.; Du, Z.; Lu, L.; Zhang, W. A Thermodynamic Reassessment of the Al-As-Ga System. *J. Phase Equilibria* **2001**, *22* (1), 26–33.

(6) Maliakkal, C. B.; Jacobsson, D.; Tornberg, M.; Persson, A. R.; Johansson, J.; Wallenberg, R.; Dick, K. A. In Situ Analysis of Catalyst Composition during Gold Catalyzed GaAs Nanowire Growth. *Nat. Commun.* **2019**, *10* (1), 4577.

(7) Yang, F.; Messing, M. E.; Mergenthaler, K.; Ghasemi, M.; Johansson, J.; Wallenberg, L. R.; Pistol, M.-E.; Deppert, K.; Samuelson, L.; Magnusson, M. H. Zn-Doping of GaAs Nanowires Grown by Aerotaxy. *J. Cryst. Growth* **2015**, *414*, 181–186.

(8) Sun, R.; Jacobsson, D.; Chen, I.-J.; Nilsson, M.; Thelander, C.; Lehmann, S.; Dick, K. A. Sn-Seeded GaAs Nanowires as Self-Assembled Radial p–n Junctions. *Nano Lett.* **2015**, *15* (6), 3757–3762.